

Solvent Accelerated Polymer Diffusion in Thin Films

Richard L. Thompson,* Martin T. McDonald, Joseph T. Lenthall, and Lian R. Hutchings

Department of Chemistry, University of Durham, South Road, Durham DH1 3LE, United Kingdom

Received February 14, 2005; Revised Manuscript Received March 15, 2005

ABSTRACT: We have investigated the absorption of cyclohexane vapor into polystyrene films and the resulting polymer interdiffusion that is enabled by this process. The swelling of films due to solvent absorption was relatively insensitive to the film thickness or polymer molecular weight but increased with increasing temperature. The interdiffusion enabled by absorbed solvent was examined in multilayered films comprising alternating layers of deuteriopolystyrene (*d*PS) and hydrogenous polystyrene (*h*PS). Deuterium concentration gradients were measured in dry films following exposure to cyclohexane vapor at controlled temperatures and times to establish the relationship between the coefficient of solvent accelerated interdiffusion, D^* , and (i) M_w of *h*PS, (ii) M_w of both *h*PS and *d*PS, (iii) temperature, and (iv) film thickness. Scaling relationships were established for D^* as a function of molecular weight, $D^* \sim M_w^{-1}$ for increasing *h*PS molecular weight for $M_w(hPS) < M_w(dPS)$ and was independent of $M_w(hPS)$ for $M_w(hPS) > M_w(dPS)$. This indicates that the lower molecular weight polymer, in keeping with predictions of “fast-mode” diffusion theory, dominates the rate of interdiffusion. When both *d*PS and *h*PS molecular weights were increased simultaneously, the interdiffusion coefficient scaled with $M_w^{-1.8}$. A marked increase in D^* with increasing solvent temperature was observed, consistent with the temperature dependence of film swelling. A strong and unexpected correlation between D^* and total film thickness was found. This effect was attributed to prolonged solvent retention in thicker films following exposure to solvent vapor.

Introduction

There is a growing interest in the use of multiple layers of polymers in thin film devices, both as device components and for the encapsulation of components.¹ Deposition methods for polymers frequently require volatile solvents, and as a result, there is serious concern that the solvent used to deposit one layer may corrupt the organization of the previously deposited components.² Solvent-induced mixing may be of benefit in instances when enhanced bonding between polymer layers is desirable. However, some applications such as photovoltaic devices require segregation between layers to achieve optimal performance.³ Clearly, a better understanding of the extent of polymer mixing induced by the absorption of solvent is important to the development of efficient multilayer devices.

The diffusion of solvents into^{4–7} and within^{8–11} polymer materials has been studied extensively. Kramer et al.^{9–11} used ion beam methods to determine the concentration profile of small-molecule diffusants into polymers and generally found good agreement between experimental results and the predictions of the Thomas and Windle model⁷ for case II diffusion. In this mechanism, a sharp front in concentration gradient between the glassy polymer and the solvated polymer forms and propagates through the polymer film at constant velocity. The rate of propagation is limited by the response of the polymer to the osmotic stress due to the penetrating solvent, and in this regime, the swelling rate of the polymer material should be constant until the film becomes saturated.

Despite the body of literature that has developed on solvent diffusion into polymers, there is relatively little data on the converse process of polymer diffusion under the influence of a penetrating solvent. This situation is

in part due to the difficulty in measuring polymer diffusion at intermediate (0.1–0.9) volume fractions.¹²

It is well established that a penetrating solvent can be used to reorganize block copolymers in ultrathin films¹³ and to reduce the surface roughness¹⁴ of polymer films. Recently, Watkins et al.¹⁵ have achieved enhanced rates of polystyrene diffusion in thin films and a reduction in the glass transition temperature by swelling the film with supercritical CO₂. The ability to reduce the glass transition in this way is particularly appealing for applications where the organization of thermally unstable polymers is required. Although supercritical CO₂ is an attractive alternative to organic solvents for some applications, others such as spin-coating films require a solvent that will evaporate without the risk of cavitation or delamination in the deposited film. While the organization¹³ and adsorption¹⁶ of polymers have been demonstrated via exposure of films to solvent vapor, we are unaware of any attempt to quantify the rate and range of this process. Here, we quantify the rate of solvent-mediated interdiffusion for this process in a model polystyrene system. In particular, we are concerned with the scaling of this behavior with molecular weight and with the impact of surfaces and interfaces on solvent accelerated polymer interdiffusion.

Experimental Section

Materials. Perdeuterated polystyrene (*d*PS) and hydrogenous polystyrene (*h*PS) were synthesized via living anionic polymerization. Molecular weight data obtained by size exclusion chromatography for each polymer are summarized in Table 1. Films of *d*PS and *h*PS were prepared on fresh silicon wafers by spin-coating from toluene solutions. Multilayer samples were prepared by spin-coating additional films of approximately equal thickness on large glass microscope slides, followed by flotation onto deionized water prior to pickup onto the original coated silicon wafer. After drying, the films were annealed at 393 K for 30 min to ensure entanglement across each interface, then aged overnight under vacuum at 363

* To whom correspondence should be addressed. E-mail: R.L.Thompson@durham.ac.uk.

Table 1. Molecular Weight Data of Polymers

polymer	$M_w/\text{kg/mol}$	M_w/M_n	polymer	$M_w/\text{kg/mol}$	M_w/M_n
dPS45	43.4	1.08	dPS230	226	1.05
hPS45	46.3	<1.05	hPS230	227	1.03
dPS75	71.0	1.08	dPS400	414	1.30
hPS75	83.8	1.14	hPS400	438	1.09
dPS140	134	1.09	hPS1000	1075	1.05
hPS140	140	1.07			

K. Aged samples were exposed to solvent vapor by placing in a sealed thermostated container with a small reservoir of cyclohexane. During this period the films swell as they absorb cyclohexane vapor. The extent of film swelling due to cyclohexane absorption was monitored using optical reflectometry. Following solvent exposure, the samples were removed from the cell, and they returned toward their original thickness within a few seconds as the cyclohexane evaporated.

Nuclear Reaction Analysis. The concentration of deuterium due to the dPS in specimens was determined as a function of depth following exposure to cyclohexane vapor using the $D(^3\text{He}^+, p)\alpha$ reaction.^{17,18} The maxima in stopping power and reaction cross-section for $^3\text{He}^+$ are both at approximately 0.7 MeV; therefore, optimal sensitivity and depth resolution were achieved by delivering the $^3\text{He}^+$ ions to the sample surface at an orientation and energy such that they had approximately 0.7 MeV remaining as they reached the dPS/hPS interface. The beam was collimated to 2 mm diameter, and samples were exposed to $5\ \mu\text{C}\ ^3\text{He}^+$ to obtain adequate statistical quality. Repeated $5\ \mu\text{C}$ measurements on the same sample spot yielded data of slightly reduced intensity but apparently identical deuterium distribution. We are therefore confident that beam damage has no influence on our analysis. Protons ejected from the samples were detected at 170° (backscattering geometry) to the incident beam. Raw data were converted to volume fraction by normalization with respect to smoothed data obtained from a thick pure dPS film. Conversion of proton energy to deuterium depth was carried out using the thick target approximation.¹⁹

Results

The aging process has been shown to be necessary by Kramer et al.^{9,10} to ensure consistent rates of penetration of solvent vapor into films. Without this pretreatment, significantly faster solvent penetration and resultant interdiffusion were observed, but with little consistency between specimens. The interfacial broadening arising from the initial annealing at 393 K was estimated using WLF calculations to be ~ 10 nm in the case of the lowest molecular weight polymers and less for the higher molecular weight polymers. Since the resolution of nuclear reaction analysis at the buried interface was 10 nm or worse, this annealing had a negligible effect on values subsequently measured for the interfacial width.

Typical optical reflectometry results in Figure 1 show that film thickness increased by approximately 50–80%, corresponding to 33–45% solvent by volume in the swollen films. The film swelling was initially quite rapid, reaching a stable “plateau” region in swollen film thickness. Assuming that case II diffusion applies to cyclohexane penetration of these films, it appears that the diffusion front traversed the entire film within the first minute of sample exposure. Data in Figure 2 show averaged values for the plateau region of film swelling as a function of film thickness. There is little influence of either polymer molecular weight or film thickness on the relative extent of swelling. For both molecular weights, the relative increase in film thickness increases with increasing temperature.

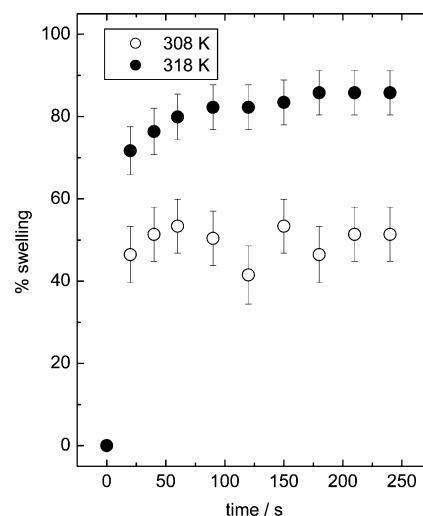


Figure 1. Extent of hPS140 film swelling in cyclohexane as a function of exposure time. The original film thickness was approximately 113 nm.

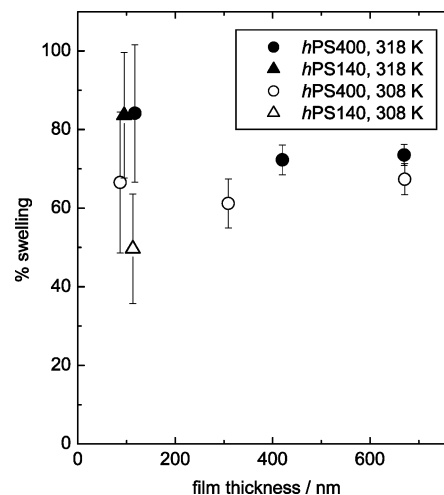


Figure 2. Extent of film swelling in cyclohexane vapor vs total film thickness and molecular weight.

Typical nuclear reaction analysis data, for a three-layer dPS/hPS/dPS film, normalized to volume fraction dPS vs depth are shown in Figure 3. The normalized data still contain the instrumental resolution convolved with the true volume fraction vs depth profile. Provided the polymer interdiffusion in the solvent-swollen films is Fickian, and approximately independent of concentration, the volume fraction of dPS, ϕ_{dPS} , may be expressed as a function of depth, x , by eq 1.

$$\phi_{dPS}(x, \forall \{0 < x < L\}) = \frac{1}{2} \left[\text{erf}\left(\frac{h_1 - x}{w_1}\right) + \text{erf}\left(\frac{h_1 + x}{w_1}\right) + \text{erf}\left(\frac{x - h_2}{w_2}\right) + \text{erf}\left(\frac{2L - h_2 - x}{w_2}\right) \right] \quad (1)$$

where L is the total film thickness, and the dPS/hPS interfaces are located at h_1 and h_2 .

Equation 1 was convolved with the depth resolution and then nonlinearly least-squares fitted to the normalized data. The fitted parameters were the interfacial widths, w_1 and w_2 , and interfacial depths, h_1 and h_2 . The interfacial depths were not displaced significantly from their original values ($L/3$ and $2L/3$) following exposure to solvent vapor. This suggests that little

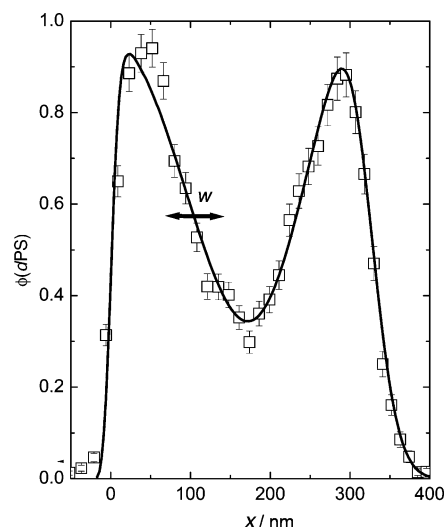


Figure 3. Normalized volume fraction vs depth data extracted from nuclear reaction analysis of a *d*PS230/*h*PS1000/*d*PS230 trilayer film. The curve of best fit to the data was obtained using eq 1 with the interfacial widths and depths as variable parameters.

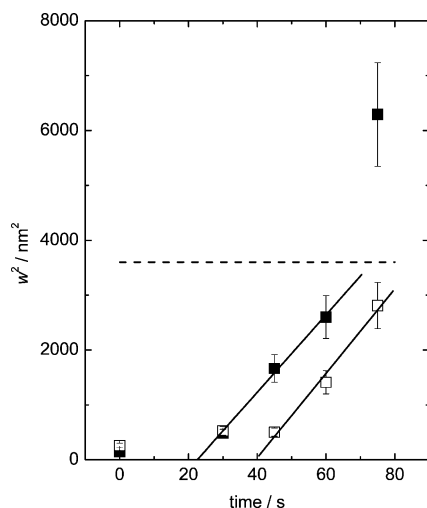


Figure 4. Growth of interfacial width at the two internal interfaces of *d*PS230/*h*PS230/*d*PS230 trilayer films vs cyclohexane vapor exposure time at 318 K. The solid and open points indicate the upper and lower interfaces, respectively. The dashed line indicates the limit in w^2 before these parameters become correlated.

solvent remained trapped within the film after removal from the cell containing solvent vapor. After a short period, both w_1 and w_2 increased with increasing exposure time to cyclohexane vapor. Data in Figure 4 clearly demonstrate that the induction period for w_2 , the deeper interface, is longer than for w_1 , showing that interdiffusion is only possible after the solvent has penetrated as far as each interface. In this case, the “induction period” between exposure to cyclohexane vapor and the commencement of interdiffusion is thought to arise from the “induction time” discussed by Thomas and Windle⁷ for the establishment of a case II diffusion front plus the propagation time for this front to reach the relevant interface.

After the induction period, the square of interfacial width grows linearly with time, indicating Fickian diffusion with a time-independent diffusion coefficient. Over the regions in which w_1^2 and w_2^2 grow linearly with increasing solvent exposure time, the slope of the

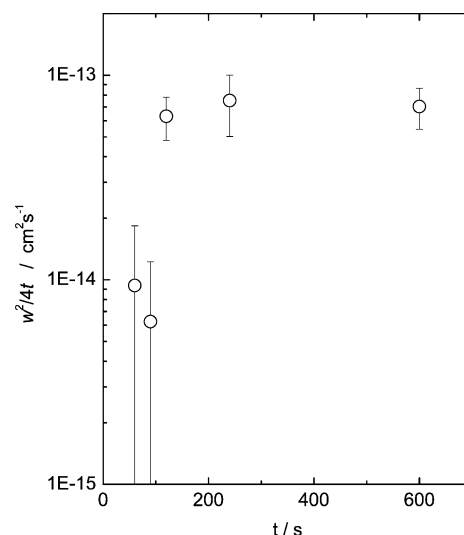


Figure 5. Instantaneous diffusion coefficient, $w^2/4t$, for *d*PS1000/*h*PS230/*d*PS1000 film as a function of exposure time to cyclohexane vapor at 318 K.

fitted lines in Figure 4 is indistinguishable, indicating that the polymer interdiffusion coefficient does not vary significantly within each sample as a function of depth. Since the accuracy of ion beam analysis data generally decreases with increasing depth due to beam straggling, the subsequent analysis will focus on w_1 values obtained at the uppermost *d*PS/*h*PS interface.

After prolonged exposure times, $w_1 + w_2$ may exceed the thickness of the intervening *h*PS layer. Beyond this point the parameters become correlated, and the interfacial width data are no longer reliable. The data in Figure 5 were obtained for a sample in which the *h*PS layer was 120 nm thick. It therefore follows that w^2 values are only reliable up to a limit of 3600 nm².

Using the relation

$$w = \sqrt{4D^*t} \quad (2)$$

where D^* is the polymer–polymer interdiffusion coefficient, an instantaneous time-dependent diffusion coefficient may be extracted from the plot of $w^2/4t$ vs t shown in Figure 5. Clearly again the induction period, during which polymer–polymer diffusion is essentially negligible, is visible, followed by a sharp rise to a constant value for D^* . Hereafter, D^* values reported were obtained from a linear regression fit to the linear region of a plot of w^2 vs $4t$. The errors shown are the uncertainty in the linear regression fit.

Figure 6 shows the molecular weight dependence for D^* in *d*PS230/*h*PS/*d*PS230 films in which $M_w(hPS)$ was varied systematically. D^* decreases linearly with increasing $M_w(hPS)$ up to the point where the molecular weight of each component in the film is equal. Further increasing $M_w(hPS)$ appears to have little effect on D^* .

The influence of varying $M_w(hPS)$ and $M_w(dPS)$ simultaneously is shown in Figure 7 at two temperatures. At both 308 and 318 K, D^* was found to scale approximately with $M_w^{-1.8}$. Diffusion at the higher temperature is more rapid by a factor of ~ 1.6 over the molecular weight range examined. It must be stressed that the diffusion coefficients compared in Figure 7 were obtained for films of identical thickness. An unexpected, but clear, dependence of D^* on total film thickness was found. Data in Figure 8 clearly demonstrate that

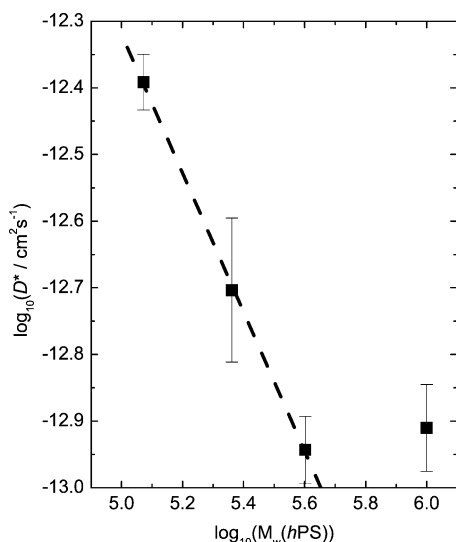


Figure 6. Dependence of *d*PS/*h*PS interdiffusion coefficient for *d*PS230 as a function of *h*PS molecular weight. The slope of the fitted curve gives $D^* \sim M_w^{-1.04 \pm 0.12}$.

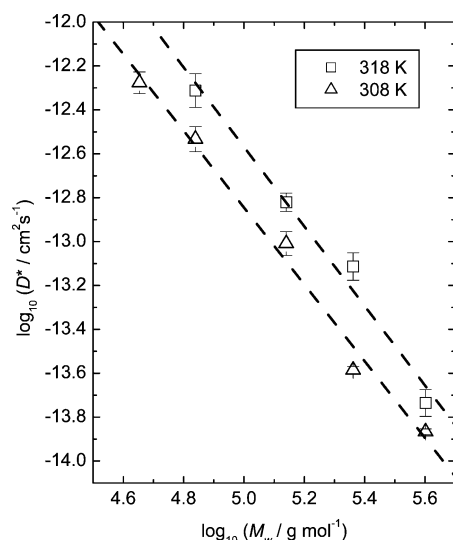


Figure 7. Diffusion coefficient vs molecular weight in 460 nm thick *d*PS/*h*PS/*d*PS trilayer films. The fitted slopes to the 308 and 318 K data indicate $D^* \sim M_w^{-1.81 \pm 0.17}$ and $D^* \sim M_w^{-1.75 \pm 0.11}$, respectively.

polymer interdiffusion coefficients increase with increasing film thickness.

Discussion

Film Swelling. The time dependence of *h*PS film swelling under the influence of cyclohexane vapor shown in Figure 1 is typical of all of the molecular weights and temperatures for which this behavior was examined. In the analysis of the reflectometry data, it was assumed that the refractive index of the solvent-swollen film was the volume fraction weighted average of the pure components. The accuracy of the optical reflectometry method used increases with increasing film thickness, hence the larger scatter in the data for the thinnest films shown in Figure 2. The relative swelling of the films is approximately independent of polymer molecular weight and film thickness, indicating that these parameters have little effect on the solvent content of the swollen film.

By increasing the temperature of solvent exposure from 308 K (close to the Θ temperature) to 318 K, both

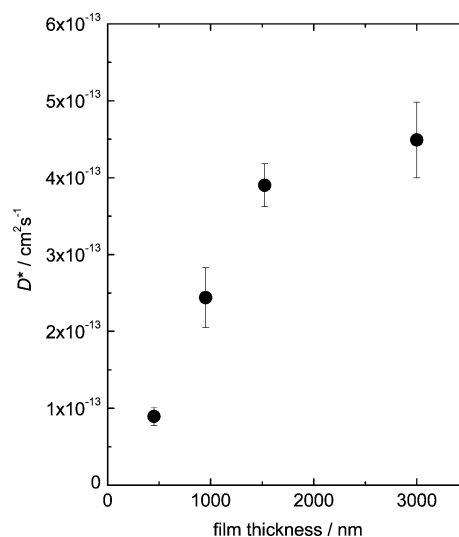


Figure 8. Variation in D^* with total film thickness for *d*PS230/*h*PS230 at 318 K.

the vapor pressure of the solvent²⁰ and the osmotic pressure of the polystyrene increase. While increasing the temperature of the film is known to increase the rate of solvent penetration,⁹ the equilibrium extent of swelling should depend only on the osmotic pressure of the film. The reason for the plateau in the swelling of the films is unclear since the films were in equilibrium with a pure solvent, and therefore a finite osmotic pressure would be expected to promote swelling (albeit at an ever decreasing rate) toward infinite dilution. One possibility is that the entangled nature of the polymer chains temporarily gives rise to the gel-like behavior in which the osmotic pressure is reduced.²¹ However, this effect would not be expected to persist beyond the characteristic relaxation time of the polymers in the swollen film and is therefore implausible given our clear evidence for long-range polymer interdiffusion on similar time scales. We believe that it is more likely that the transport of vapor to the film is limited either through the depletion of solvent vapor from the headspace above the film caused by temperature gradients within the sample cell or the heat of condensation of vapor onto the film. While it is not possible to resolve these effects using the current apparatus, we note that the solvent diffusion experiments of Kramer et al. showed similar behavior. In their experiments, the maximum volume fraction of toluene¹¹ and iodoheptane^{9,10} in solvent-swollen polystyrene films appeared to be consistently somewhat less than the solvent volume fraction of the solutions used to swell the film.

The correlation between solvent penetration of the polymer films and polymer interdiffusion is illustrated by the differing induction periods shown for the growth of each internal interface of a three-layer film in Figure 4. The lag in induction time between the two interfaces is consistent with a case II diffusion front of cyclohexane passing through the film at a rate of ≈ 8 nm/s.

Polymer Interdiffusion. Influence of Molecular Weight on D^* . Figure 6 shows that while D^* decreases with increasing $M_w(hPS)$ for $M_w(hPS) < M_w(dPS)$, there is little effect of increasing *h*PS molecular weight beyond that of the *d*PS. This implies that solvent accelerated polymer diffusion is dominated by the diffusion coefficient of the lower molecular weight polymer. Such behavior is already well established for the melt diffu-

sion of polymers in thin films²² and is predicted by the “fast mode” polymer diffusion theories.^{23,24} To our knowledge, this is the first evidence presented for this diffusion mechanism between polymers of differing molecular weight facilitated by the presence of a third component. Inherent to this mode of diffusion is the requirement that the flux of each component across the interface is unequal. We note that the presence of a third, highly mobile component in the blend could assist in this process.

The entanglement molecular weight of polystyrene swollen by a low molecular weight solvent is given by the relation $M_e = 18000/c$, where c is the polystyrene concentration.¹⁵ For the solvent-swollen polymer films, c varies from 0.55 to 0.67, giving rise to a maximum M_e value of 35 000 g/mol. All of the polymer systems examined here exceed the entanglement weight, and therefore D^* is expected to approximate to the M_w^{-2} dependence predicted for the reptation of a polymer chain in a high molecular weight matrix. The discrepancy between this prediction and the observed molecular weight dependence in Figure 6 is easily resolved when one considers that two d PS layers of invariant molecular weight surround the interstitial h PS layer. In these systems, the diffusion coefficient measured is due to the interdiffusion between both of these components.

When the molecular weight of each layer of the diffusion couple was varied simultaneously, the results in Figure 7 more closely approximated the behavior expected for reptating polymer chains. Strictly speaking, the finite molecular weight of the matrix should yield an exponent that is somewhat greater than 2 due to constraint release and contour length fluctuation effects.²⁵ The measured scaling exponent of 1.8 suggests that the situation is skewed by some additional factor that increases the apparent rate of interdiffusion in the highest molecular weight polymer films. The interdiffusion coefficients reported here are based on the rate of growth of interfacial width after the induction period but may be anomalously high when one takes into account the finite period required for the solvent to leave the film after removal from the solvent vapor. The observed M_w dependence could be explained if the ability of films to retain solvent increases with increasing polymer molecular weight.

Temperature Dependence of D^* . Attempts were made to characterize polymer interdiffusion in films exposed to cyclohexane vapor at 298, 308, 318, and 328 K. At 298 K, interdiffusion was extremely slow, and it was not possible to obtain consistent data. The d PS and h PS of the layers of the film became fully mixed within the first 30 s of exposure to cyclohexane at 328 K. Data for the two intermediate temperatures in Figure 7 show an increase in D^* with increasing temperature. This result was expected since the rate of cooperative diffusion of linear polystyrenes has been shown to increase with increasing temperature.¹² Moreover, the concentration of polymer within the actual film will decrease with increasing temperature as a direct consequence of the increased swelling of the film. Thus, despite the insensitivity of the polymer dimensions to cyclohexane temperature in the concentrated regime,²⁶ the number of entanglements per polymer chain in swollen films decreases with increasing temperature. To separate the factors contributing to the observed temperature dependence of D^* , it would be necessary to control the

sample temperature and cyclohexane vapor pressure independently.

Influence of Film Thickness on D^* . Although it is well-known^{27,28} that the melt mobility of polymer chains in the vicinity of surfaces and interfaces differs significantly from the bulk value, these effects are normally limited in their range. Sokolov et al.²⁸ have reported that surface D^* can be reduced with respect to the bulk value as far as $10R_g$ from the substrate interface, corresponding to the minimum film thickness prior to swelling examined in this study. We found no clear dependence of film swelling on the total film thickness, and interdiffusion coefficients measured for dry films annealed above their T_g were in good agreement with literature values. It was therefore surprising to find that D^* values were strongly dependent on L over the range for which ion beam analysis could be used to determine diffusion coefficients. The result suggests that a small fraction of cyclohexane remains following the solvent annealing process in all but an upper crust of the film. De Gennes predicted the presence of a “crust” on the surface of spin-coated films that develops during the evaporation of the solvent.²⁹ Similar behavior has also been demonstrated for solvent evaporation in polymer films above their glass transition via molecular dynamics simulations.³⁰ In de Gennes’ model of crust formation, a near-surface region, from which solvent evaporation was initially rapid, reduces the rate of evaporation from the deeper parts of the film. This in turn may allow further polymer interdiffusion to occur after removal of the sample from the solvent reservoir, to an extent that increases with increasing film thickness. Critically, the predicted lifetime of the crust before the entire film beneath becomes glassy is proportional to L . The thickness of the crust, b^* , is given by eq 3

$$b^* = l \frac{p_a D(\psi^*)}{p_v v_{th} a} \quad (3)$$

where l is the depth of the region of air over which the solvent vapor concentration varies; p_a and p_v are the atmospheric and solvent partial vapor pressures, respectively. $D(\psi^*)$ is the diffusion coefficient of the solvent in the polymer, v_{th} is the thermal velocity of the solvent molecule, and a is its characteristic size. Using this approach, we arrive at a nominal crust thickness for the PS–cyclohexane system of the order of a few nanometers. Notwithstanding the uncertainty in the values of l and $D(\psi^*)$ used in the calculation, it is likely that b^* is thinner than the uppermost d PS film in all of our experimental systems. We note that this prediction is consistent with the observed behavior in Figure 4. If the crust thickness exceeded the thickness of the upper layer of the film, widely differing growth rates of w_1 and w_2 might be expected.

Conclusions

We have described the swelling of polystyrene films via the absorption of cyclohexane vapor and the resulting polymer interdiffusion that occurs in the swollen films. When placed in equilibrium with a small reservoir of pure cyclohexane, all of the polystyrene films rapidly became swollen until a state that was at least metastable was attained, typically containing 33–45% cyclohexane. The extent of swelling increased with increasing temperature but was relatively insensitive to both total film thickness and molecular weight.

The interdiffusion between *d*PS and *h*PS layers in films was determined using $^3\text{He}^+$ nuclear reaction analysis. After a brief induction period, thought to correspond to the propagation of a case II diffusion front, polymer interdiffusion occurred at a rate that was independent of depth within the film. The rate of interdiffusion was found to increase significantly with increasing temperature, consistent with the dilution increasing with increasing film swelling. Polymer interdiffusion appeared to scale with inverse molecular weight when the molecular weight of just one polymer component was varied, while being independent of the molecular weight of the higher molecular weight component. This suggests that the fast-mode theory of polymer diffusion may be appropriate to describe solvent accelerated polymer diffusion. When the molecular weight of both *h*PS and *d*PS were varied simultaneously, diffusion scaled with $M_w^{-1.8}$, closer to the anticipated result for entangled polymer chains. The rate of polymer interdiffusion appeared to be remarkably sensitive to total film thickness, indicating that surfaces and interfaces may play a significant role in solvent accelerated polymer interdiffusion. The increase in D^* with increasing film thickness is consistent with some residual solvent remaining in the films and allowing interdiffusion to occur after removal from the solvent vapor source. This effect could also be responsible for the small discrepancy between observed and anticipated ($M_w^{-2.3}$) and measured ($M_w^{-1.8}$) dependence of D^* . Recent theoretical predictions of de Gennes were used to estimate the probable crust thickness of the polymer film as the solvent evaporated. The crust thickness was predicted to be much thinner than the uppermost layer of the polymer films and is therefore consistent with the equal growth rates for w_1 and w_2 and the increase in D^* with increasing L and M_w .

Acknowledgment. The authors are grateful to the Nuffield Foundation for the provision of an Undergraduate Research Bursary (URB/01459/G) to support this work.

References and Notes

- (1) MacDonald, W. A. *J. Mater. Chem.* **2004**, *14*, 4–10.
- (2) Domercq, B.; Hreha, R. D.; Zhang, Y.-D.; Larribeau, N.; Haddock, J. N.; Schultz, C.; Marder, S. R.; Kippelen, B. *Chem. Mater.* **2003**, *15*, 1491–1496.
- (3) Chappell, J.; Lidzey, D. G.; Jukes, P. C.; Higgins, A. M.; Thompson, R. L.; O'Connor, S.; Grizzi, I.; Fletcher, R.; O'Brien, J.; Geoghegan, M.; Jones, R. A. L. *Nat. Mater.* **2003**, *2*, 616–621.
- (4) Vrentas, J. S.; Vrentas, C. M. *J. Appl. Polym. Sci.* **2003**, *89*, 2778–2779.
- (5) Vrentas, J. S.; Vrentas, C. M. *Macromolecules* **1993**, *26*, 6129–6131.
- (6) Vrentas, J. S.; Chu, C. H. *J. Polym. Sci., Part B: Polym. Phys.* **1989**, *27*, 465–468.
- (7) Thomas, N. L.; Windle, A. H. *Polymer* **1982**, *23*, 529–542.
- (8) Umezawa, K.; Gibson, W. M.; Welch, J. T.; Araki, K.; Barros, G.; Frisch, H. L. *J. Appl. Phys.* **1992**, *71*, 681–684.
- (9) Lasky, R. C.; Kramer, E. J.; Hui, C. Y. *Polymer* **1988**, *29*, 1131–1136.
- (10) Lasky, R. C.; Kramer, E. J.; Hui, C. Y. *Polymer* **1988**, *29*, 673–679.
- (11) Gall, T. P.; Kramer, E. J. *Polymer* **1991**, *32*, 265–271.
- (12) Nicolai, T.; Brown, W. *Macromolecules* **1996**, *29*, 1698–1704.
- (13) Konrad, M.; Knoll, A.; Krausch, G.; Magerle, R. *Macromolecules* **2000**, *33*, 5518–5523.
- (14) Anthamatten, M.; Letts, S. A.; Cook, R. C. *Langmuir* **2004**, *20*, 6288–6296.
- (15) Gupta, R. R.; Lavery, K. A.; Francis, T. J.; Webster, J. R. P.; Smith, G. S.; Russell, T. P.; Watkins, J. J. *Macromolecules* **2003**, *36*, 346–352.
- (16) Kiff, F. T.; Richards, R. W.; Thompson, R. L. *Langmuir* **2004**, *20*, 4465–4470.
- (17) Payne, R. S.; Clough, A. S.; Murphy, P.; Mills, P. J. *Nucl. Inst. Methods Phys. Res. B* **1989**, *42*, 130–134.
- (18) Chaturvedi, U. K.; Steiner, U.; Zak, O.; Krausch, G.; Schatz, G.; Klein, J. *Appl. Phys. Lett.* **1990**, *56*, 1228–1230.
- (19) Composto, R. J.; Walters, R. M.; Genzer, J. *Mater. Sci. Eng. R* **2002**, *R38*, 107–180.
- (20) Timmermans, J. *Physico-Chemical Constants of Pure Organic Compounds*; Elsevier: Amsterdam, 1965; Vol. 2.
- (21) Hecht, A. M.; Guillermo, A.; Horkay, F.; Mallam, S.; Legrand, J. F.; Geissler, E. *Macromolecules* **1992**, *25*, 3677–3684.
- (22) Reiter, G.; Huttenbach, S.; Foster, M.; Stamm, M. *Macromolecules* **1991**, *24*, 1179–1184.
- (23) Sillescu, H. *Makromol. Chem., Rapid Commun.* **1984**, *5*, 519–523.
- (24) Kramer, E. J.; Green, P.; Palmstrom, C. J. *Polymer* **1984**, *25*, 473–480.
- (25) Lodge, T. P. *Phys. Rev. Lett.* **1999**, *83*, 3218–3221.
- (26) Cotton, J. P.; Nierlich, M.; Boue, F.; Daoud, M.; Farnoux, B.; Jannink, G.; Duplessix, R.; Picot, C. *J. Chem. Phys.* **1976**, *65*, 1101–1108.
- (27) Jones, R. A. L. *Curr. Opin. Colloid Interface Sci.* **1999**, *4*, 153–158.
- (28) Zheng, X.; Rafailovich, M. H.; Sokolov, J.; Strzhemechny, Y.; Schwarz, S. A.; Sauer, B. B.; Rubinstein, M. *Phys. Rev. Lett.* **1997**, *79*, 241–244.
- (29) de Gennes, P. G. *Eur. Phys. J. E* **2002**, *7*, 31–34.
- (30) Tsige, M.; Grest, G. S. *Macromolecules* **2004**, *37*, 4333–4335.

MA050317P